

Accepted for publication in the Astrophysical Journal

A photometric survey for Ly α -He II dual emitters: Searching for Population III stars in high-redshift galaxies

Tohru Nagao ¹, Shunji S. Sasaki ^{2,3}, Roberto Maiolino ⁴, Celestine Grady ⁵,
Nobunari Kashikawa ¹, Chun Ly ⁵, Matthew A. Malkan ⁵, Kentaro Motohara ⁶,
Takashi Murayama ², Daniel Schaerer ⁷, Yasuhiro Shioya ^{3,8}, Yoshiaki Taniguchi ^{3,8}

ABSTRACT

We present a new photometric search for high- z galaxies hosting Population III (PopIII) stars based on deep intermediate-band imaging observations obtained in the Subaru Deep Field (SDF), by using Suprime-Cam on the Subaru Telescope. By combining our new data with the existing broad-band and narrow-band data, we searched for galaxies which emit strongly both in Ly α and in He II λ 1640 (“dual emitters”) that are promising candidates for PopIII-hosting galaxies, at $3.93 \lesssim z \lesssim 4.01$ and $4.57 \lesssim z \lesssim 4.65$. Although we found 10 “dual emitters”, most of them turn out to be [O II]-[O III] dual emitters or H β -(H α + [N II]) dual emitters at $z < 1$, as inferred from their broad-band colors and from the ratio of the equivalent widths. No convincing candidate of Ly α -He II dual emitter of $SFR_{\text{PopIII}} \gtrsim 2M_{\odot} \text{ yr}^{-1}$ was found by our photometric search in $4.03 \times 10^5 \text{ Mpc}^3$ in the SDF. This result disfavors low feedback models for PopIII star clusters, and implies an upper-limit of the PopIII SFR density of $SFRD_{\text{PopIII}} < 5 \times 10^{-6} M_{\odot} \text{ yr}^{-1} \text{ Mpc}^{-3}$. This new selection method to search for PopIII-hosting galaxies should be useful in future narrow-band surveys to achieve the first observational detection of PopIII-hosting galaxies at high redshifts.

¹ National Astronomical Observatory of Japan, 2-21-1 Osawa, Mitaka, Tokyo 181-8588, Japan

² Astronomical Institute, Graduate School of Science, Tohoku University, Aramaki, Aoba, Sendai 980-8578, Japan

³ Department of Physics, Graduate School of Science and Engineering, Ehime University, 2-5 Bunkyo-cho, Matsuyama 790-8577, Japan

⁴ INAF – Osservatorio Astrofisico di Roma, Via di Frascati 33, 00040 Monte Porzio Catone, Italy

⁵ Department of Physics and Astronomy, University of California at Los Angeles, P. O. Box 951547, Los Angeles, CA 90095-1547, USA

⁶ Institute of Astronomy, Graduate School of Science, University of Tokyo, 2-21-1 Osawa, Mitaka, Tokyo 181-0015, Japan

⁷ Geneva Observatory, University of Geneva, 51 chemin des Maillettes, 1290 Sauverny, Switzerland

⁸ Research Center for Space and Cosmic Evolution, Ehime University, 2-5 Bunkyo-cho, Matsuyama 790-8577, Japan

Subject headings: early universe – galaxies: evolution – galaxies: formation – galaxies: starburst – stars: early-type

1. Introduction

Population III (PopIII) stars are those formed out of primordial gas, enriched only through Big-Bang nucleosynthesis. Since massive PopIII stars are promising candidates as sources for cosmic reionization (e.g., Ciardi et al. 2000; Loeb & Barkana 2001; Wyithe & Loeb 2003; Sokasian et al. 2004) and an important population for early phases of the cosmic chemical evolution (e.g., Wasserburg & Qian 2000; Abia et al. 2001; Qian & Wasserburg 2001; Bromm et al. 2003), their properties have been extensively investigated from the theoretical point of view. PopIII stars have not been discovered yet; obviously, their direct detection and the observational studies of their properties would provide a completely new and important step toward understanding the evolution of galaxies. The expected observables of high- z galaxies hosting PopIII stars have been theoretically investigated in recent years. Such galaxies are expected to show strong Ly α emission, with an extremely large equivalent width (EW), and moderately strong He II λ 1640 emission (e.g., Tumlinson & Shull 2000; Tumlinson et al. 2001; Oh et al. 2001; Schaerer 2002, 2003; Tumlinson et al. 2003), due to the high effective temperature up to $\sim 10^5$ K of PopIII stars (e.g., Bromm et al. 2001; Tumlinson et al. 2003).

Most models predict that PopIII stars dominated the re-ionization of the universe at $7 \lesssim z \lesssim 15$. However, they also predict that PopIII stars may still exist at redshifts currently accessible with 8 – 10m-class telescopes, i.e., $z < 7$, although it may depend both on some model parameters of PopIII [e.g., initial mass function (IMF)] and on some environmental parameters such as the mixing efficiency (e.g., Scannapieco et al. 2003, 2006; Jimenez & Haiman 2006; Schneider et al. 2006; Brook et al. 2007; Tornatore et al. 2007). Some observations have found Ly α emitters (LAEs) at $z > 4$ with a very large EW, which is hard to explain through star-formation without PopIII (e.g., Malhotra & Rhoads 2002; Nagao et al. 2004, 2005a, 2007; Shimasaku et al. 2006; Dijkstra & Wyithe 2006). However, the search for He II λ 1640 emission as direct evidence for the presence of PopIII in such galaxies is far more controversial. Jimenez & Haiman (2006) pointed out the possible He II λ 1640 signature in the composite spectrum of ~ 1000 Lyman-break galaxies (LBGs) at $z \sim 3$ made by Shapley et al. (2003), although the He II λ 1640 feature in the LBG composite spectrum may be attributed to a stellar wind feature associated with massive stars as mentioned by Shapley et al. (2003). On the other hand, other searches for He II λ 1640 in higher- z galaxies have failed, through stacking analysis of LAEs (Dawson et al. 2004; Ouchi et al. 2008) or through ultra-deep near-infrared spectroscopy of an individual LAE (Nagao et al. 2005b).

Nevertheless, the He II λ 1640 emission from PopIII-hosting galaxies may already be detected in current deep narrow-band (NB) surveys (mostly aiming for LAE searches) as NB-excess objects, but not identified as He II emitters (Tumlinson et al. 2001) since NB surveys are more sensitive to faint emission lines than spectroscopic observations. Galaxies in a young PopIII-hosting phase are

expected to show He II $\lambda 1640$ emission with $EW_{\text{rest}} > 20\text{\AA}$ (e.g., Schaerer 2003), which corresponds to a redshifted emission line at $\sim 9200\text{\AA}$ with $EW_{\text{obs}} > 110\text{\AA}$ for galaxies at $z \sim 4.6$. Such He II-emitting galaxies could already be present as NB-excess objects in current deep NB surveys for LAEs at $z \sim 6.5$ (see, e.g., Taniguchi et al. 2005a; Kashikawa et al. 2006). If a NB-excess object is due to He II $\lambda 1640$ emission, then the same object should show stronger Ly α emission at a shorter wavelength, since the PopIII-hosting galaxies should emit Ly α with $EW_{\text{rest}} > 500\text{\AA}$ (e.g., Schaerer 2003). Therefore, by performing additional NB (or intermediate-band) imaging observations whose wavelength is matched to the redshifted Ly α , we may be able to find “Ly α -He II dual emitters” that are promising candidates for PopIII-hosting galaxies. Motivated by these considerations, we performed new intermediate-band imaging observations on the Subaru Deep Field (SDF; Kashikawa et al. 2004), where very deep and wide broad-band and NB imaging data are available¹.

In this paper, we report new intermediate-band imaging observations for the SDF, describe the combination of the new data with existing data to search for Ly α -He II dual emitters at $z \sim 4.0$ and ~ 4.6 , and discuss the inferred constraints on the population of PopIII-hosting galaxies. Throughout this paper, we adopt a cosmology with $(\Omega_{\text{tot}}, \Omega_{\text{M}}, \Omega_{\Lambda}) = (1.0, 0.3, 0.7)$ and $H_0 = 70 \text{ km s}^{-1} \text{ Mpc}^{-1}$. We use the AB photometric system for optical magnitudes.

2. Data

2.1. Method and filter selection

The field investigated in this project is the SDF, centered at $\alpha(\text{J2000}) = 13:24:38.9$ and $\delta(\text{J2000}) = +27:29:25.9$ (Kashikawa et al. 2004), where the Galactic dust extinction is low ($E_{B-V} = 0.017$ mag; Schlegel et al. 1998). The optical photometric data obtained in the SDF so far are summarized in Table 1. Among the 5 existing NB images, we focus on the NB816 and NB921 data to search for the putative He II $\lambda 1640$ emission from PopIII-hosting galaxies. Note that the central wavelengths and the half-widths of the transmittance of NB816 and NB921 are $(\lambda_{\text{c}}, \Delta\lambda_{\text{FWHM}}) = (8150\text{\AA}, 120\text{\AA})$ and $(9196\text{\AA}, 132\text{\AA})$, respectively. We did not consider the NB973 data, which are too shallow to search for He II $\lambda 1640$ emission from PopIII-hosting galaxies. We also did not use the NB704 and NB711 data, because their wavelengths are too blue, resulting in too low redshifts ($z \sim 3.3$ for He II $\lambda 1640$ emitters). The NB816 and NB921 filters can be used to search for He II $\lambda 1640$ emitters at $3.93 \lesssim z \lesssim 4.01$ or $4.57 \lesssim z \lesssim 4.65$, respectively. If there are He II $\lambda 1640$ emitters in these redshift ranges, they should show very strong Ly α emission at $5992\text{\AA} \lesssim \lambda_{\text{obs}} \lesssim 6089\text{\AA}$ or $6769\text{\AA} \lesssim \lambda_{\text{obs}} \lesssim 6867\text{\AA}$. We then used two intermediate-passband filters (“IA filter system”; see, e.g., Yamada et al. 2005; Taniguchi et al. 2005b), whose wavelengths correspond to these Ly α observed wavelengths with broader transmission FWHM than NB filters. Specifically, we used IA598 and IA679, whose central wavelengths and half-widths of transmittance are $(\lambda_{\text{c}}, \Delta\lambda_{\text{FWHM}})$

¹ The reduced data and the object catalogs are available at <http://soaps.naoj.org/>.

$= (6008\text{\AA}, 298\text{\AA})$ and $(6782\text{\AA}, 339\text{\AA})$, respectively. Note that the wide IA filters select LAEs with a very large EW (e.g., Fujita et al. 2003a; Ajiki et al. 2004; Yamada et al. 2005). This is not a problem for this project, since PopIII-hosting galaxies are expected to show Ly α emission with a very large EW ($EW_{\text{rest}} > 100\text{\AA}$; e.g., Schaerer 2002, 2003; Scannapieco et al. 2003).

In summary, we can select “Ly α -He II dual emitters” at $3.93 \lesssim z \lesssim 4.01$ by combining the IA598 and NB816 data, and at $4.57 \lesssim z \lesssim 4.65$ by combining the IA679 and NB921 data. In Figure 1, a schematic view of this selection method is shown. The target redshift ranges are shown more clearly in Figure 2, where the IA and NB filter transmission curves are shown as functions of the targeted redshift.

2.2. Observations and the data reduction

The SDF was observed on 22 April 2007 (UT) with Suprime-Cam [that has a field-of-view (FOV) of 34×27 arcmin²; Miyazaki et al. 2002] on the Subaru Telescope (Iye et al. 2004). We used two intermediate-passband filters, IA598 and IA679, as described above. The individual exposure time was 120 seconds or 900 seconds. A small dithering was performed between individual exposures to cover the gaps between the detectors and the bad pixels. The typical seeing during the observation was $0.6 - 0.9$ arcsec in FWHM. We discarded frames with bad seeing (two 900 seconds frames for each filter); as a consequence, the total integration times used to construct the final combined images of the IA598 and IA679 data are 111 minutes and 231 minutes, respectively (Table 1). We also observed spectrophotometric standard stars, G93-48, GD108, HZ21, and HZ44 for the flux calibration.

The individual CCD data were reduced and combined by using the data reduction package SDFRED (Yagi et al. 2002; Ouchi et al. 2004). Since the PSF sizes of the reduced and combined IA598 and IA679 data (0.91 arcsec and 0.93 arcsec in FWHM, respectively) are smaller than that of the existing SDF imaging data (0.99 arcsec), we matched the PSF of the IA598 and IA679 data to the existing SDF data by smoothing with proper Gaussian kernels. After masking the low-quality regions, such as the edge of the FOV and the regions affected by bright stars, the effective surveyed area is 875 arcmin². Consequently, the co-moving survey volume at $3.93 \lesssim z \lesssim 4.01$ is 2.08×10^5 Mpc³ and 1.95×10^5 Mpc³ at $4.57 \lesssim z \lesssim 4.65$; the total volume surveyed by this study is thus 4.03×10^5 Mpc³.

2.3. Source detection and photometry

By using the final images we extracted the IA598-selected and IA679-selected object catalogs. Source detection and photometry were performed by using SExtractor version 2.3.2 (Bertin & Arnouts 1996). We adopted criteria of 5 adjacent pixels and 2σ above the noise level for source detection. Photometry was performed with a 2 arcsec diameter aperture for each band image. The

3σ limiting magnitudes of IA598 and IA679 for 2 arcsec apertures are 26.52 mag and 27.07 mag, respectively (Table 1). In the following sections we used the inferred photometric catalogs with a correction for the Galactic reddening of $E_{B-V} = 0.017$ mag (Schlegel et al. 1998), adopting the extinction curve by Cardelli et al. (1989).

3. Results

3.1. Selection of IA-excess objects

To select objects with excess emission in the IA filters (“IA-excess” objects), we determined the matched continuum magnitudes for IA598 and IA679, which will be identified as C598 and C679, hereafter. They are obtained by $f_{C598} = 0.45f_V + 0.55f_{R_C}$ and $f_{C679} = 0.75f_{R_C} + 0.25f_{i'}$ respectively, where f_X is the flux density at band X. The weighting factors used here are calculated by taking the effective wavelengths of the related filters into account. The 3σ limiting magnitudes of C598 and C679 are estimated to be 27.77 mag and 27.70 mag respectively, without correction for Galactic extinction. We then selected IA598-excess objects as those matching *all* of the following criteria:

$$21.0 < IA598 < 26.52 \quad [= 3\sigma], \quad (1)$$

$$R_C > 28.24 \quad [= 2\sigma], \quad (2)$$

$$i' > 27.87 \quad [= 2\sigma], \quad (3)$$

$$C598 - IA598 > 0.3, \quad (4)$$

$$C598 - IA598 > 3\sigma(C598 - IA598), \quad (5)$$

and similarly IA679-excess objects were selected as those matching *all* of the following criteria:

$$21.0 < IA679 < 27.07 \quad [= 3\sigma], \quad (6)$$

$$R_C > 28.24 \quad [= 2\sigma], \quad (7)$$

$$i' > 27.87 \quad [= 2\sigma], \quad (8)$$

$$C679 - IA679 > 0.3, \quad (9)$$

$$C679 - IA679 > 3\sigma(C679 - IA679). \quad (10)$$

The bright-end limit of the IA magnitudes for the selection was introduced to avoid saturation and/or non-linearity effects. The IA-excess magnitude adopted here (0.3 mag) corresponds to a selection limit in terms of EW of $EW_{\text{obs}} \gtrsim 114\text{\AA}$ for IA598, and $EW_{\text{obs}} \gtrsim 145\text{\AA}$ for IA679.

Note that the adopted limiting EWs are much lower than intrinsic EWs theoretically expected for PopIII-hosting galaxies [$EW_{\text{rest}}(\text{Ly}\alpha) \gtrsim 100\text{\AA}$, which corresponds to $EW_{\text{obs}}(\text{Ly}\alpha) \gtrsim 500\text{\AA}$]. However, even in low dust-abundance environments, Ly α photons from H II regions could suffer

from resonance scattering through the neutral hydrogen and accordingly the surface brightness of the Ly α emission could be diminished, resulting in lower observed EWs. Taking this possibility into account, we set the limiting IA-excess magnitude (i.e., the limiting EWs) as described above.

In Figures 3 and 4, we show the selected IA598-excess and IA679-excess objects on the diagram of $C598 - IA598$ vs. $IA598$ and that of $C679 - IA679$ vs. $IA679$. The numbers of selected IA598-excess objects and of IA679-excess objects are 133 and 234, respectively.

3.2. Selection of IA-NB dual emitters

The IA-excess selected samples also include low- z objects, not only LAEs we are focusing on. More specifically, the IA598-excess objects may contain [O III] emitters at $z \sim 0.20$, H β emitters at $z \sim 0.24$ and [O II] emitters at $z \sim 0.61$. IA679-excess objects may contain H α (+ [N II]) emitters at $z \sim 0.03$, [O III] emitters at $z \sim 0.35$, H β emitters at $z \sim 0.40$ and [O II] emitters at $z \sim 0.82$. Note that fainter emission lines, such as [Ne III] and higher-order Balmer lines, are expected to be excluded from the IA-excess object samples, since we are sensitive only to relatively high-EW objects ($EW_{\text{obs}} \gtrsim 100\text{\AA}$).

Generally, such low- z interlopers should be removed before analyzing any statistical properties of high- z LAEs (see, e.g., Ajiki et al. 2003). However, we are now focusing on “IA-NB dual emitters” as candidates for “Ly α -He II dual emitters” (i.e., PopIII-hosting galaxies). Since low- z H α and [O III] emitters do not show any emission-line features around corresponding NB wavelengths ($\sim 8150 \pm 60\text{\AA}$ for IA598 emitters and $\sim 9196 \pm 66\text{\AA}$ for IA679 emitters), IA598-NB816 dual emitters and IA679-NB921 dual emitters do not contain them. The possible low- z contamination in IA-NB dual emitter samples is from [O II]-[O III] dual emitters and H β -(H α + [N II]) dual emitters, because the wavelength ratios of Ly α /He II, [O II]/[O III], and H β /H α are so similar (~ 0.741 , ~ 0.744 , and ~ 0.741 , respectively). More specifically, [O III] emitters observed as NB816 and NB921 emitters are at $0.62 \lesssim z \lesssim 0.64$ and $0.82 \lesssim z \lesssim 0.85$, which show [O II] emission at $6020\text{\AA} \lesssim z \lesssim 6110\text{\AA}$ and $6800\text{\AA} \lesssim z \lesssim 6890\text{\AA}$ that are covered by the IA598 and IA679 filters respectively, as shown in Figure 5. Similarly, H α (+ [N II]) emitters observed as NB816 and NB921 emitters are at $0.23 \lesssim z \lesssim 0.25$ and $0.39 \lesssim z \lesssim 0.41$, which show H β emission at $5990\text{\AA} \lesssim z \lesssim 6080\text{\AA}$ and $6760\text{\AA} \lesssim z \lesssim 6860\text{\AA}$ that are covered by the IA598 and IA679 filters respectively, as shown in Figure 5. Therefore, we select IA-NB dual emitters at first, and then will classify them into Ly α -He II, [O II]-[O III], and H β -(H α + [N II]) dual emitters.

In Figures 6 and 7, we investigate possible NB816 excesses of IA598-excess objects in the diagram of $C816 - NB816$ vs. $NB816$, and possible NB921 excesses of IA679-excess objects in the diagram of $z' - NB921$ vs. $NB921$, respectively. Here the matched continuum for NB816, C816, is defined as $f_{C816} = 0.62f_{I'} + 0.38f_{z'}$. The 3σ limiting magnitude of C816 is 27.05 mag, before Galactic reddening correction. We use the z' -band magnitude as the continuum for NB921. Note that there are +0.10 mag and -0.05 mag offsets in the color ($C816 - NB816$ and $z' - NB921$, respectively)

distribution of the detected objects, as mentioned also by Ly et al. (2007). By requiring a minimum NB816 excess of 0.3 mag (i.e., $C816 - NB816 > 0.3$, that corresponds to $EW_{\text{obs}} \gtrsim 45\text{\AA}$), there are 3 IA598-NB816 dual-excess objects with an NB816 excess significant at higher than 3σ , and 1 other IA598-NB816 dual-excess object with an NB816 excess significance higher than 2σ (Figure 6). Adopting a minimum NB921 excess of 0.15 mag (i.e., $z' - NB921 > 0.15$, that corresponds to $EW_{\text{obs}} \gtrsim 20\text{\AA}$), there are 6 IA679-NB921 dual-excess objects with a significance of the NB921 excess larger than 3σ . There are no IA679-NB921 dual-excess objects with a significance of the NB921 excess between 2σ and 3σ (Figure 7).

3.3. Selection of Ly α -He II dual emitters

In Table 2, we give the photometric properties of the 4 IA598-NB816 dual-excess objects and of the 6 IA679-NB921 dual-excess objects. Their spectral energy distributions (SEDs) are shown in Figures 8 and 9, respectively. Except for a faint IA598-NB816 dual-excess object, IA598_117217 (the only object with an NB-excess significance below 3σ), the photometric properties of all of the IA-NB dual-excess objects are apparently inconsistent with the interpretation that they are Ly α -He II dual emitters at $4.0 \lesssim z \lesssim 4.6$. This is because the IA-NB dual-excess objects show relatively blue $B - V$ colors, unlike star-forming galaxies at $z \gtrsim 4$, which are expected to have B fluxes reduced by Lyman absorption. In Figure 10, the predicted $B - V$ colors of galaxy spectral models in the observed frame are plotted as functions of redshift. We have used the galaxy SED models by Bruzual & Charlot (2003) combined with the cosmic transmission by Madau et al. (1996). The galaxy models are selected to have solar ($Z = Z_{\odot}$) or sub-solar ($Z = 0.005Z_{\odot}$) metallicity, a Salpeter IMF, and an exponentially declining star-formation history with $\tau = 1$ Gyr. It is clear that galaxies at $z \sim 4.0$ are expected to have $B - V \sim 1.8$, or even redder if dust reddening effects and the contribution of Ly α photons to the V-band flux are taken into account. Galaxies at $z \sim 4.6$ are expected to have $B - V > 3$, due to the dropout of B-band flux caused by redshifted Lyman-limit absorption at $912(1+z)\text{\AA} \sim 5100\text{\AA}$.

The three IA598-NB816 dual-excess objects (again except for IA598_117217) show $B - V \sim 0.4$, that is consistent with the interpretation that they are star-forming galaxies at $z < 1$. All of the six IA679-NB921 dual-excess objects show $-0.1 \lesssim B - V \lesssim +0.8$, again consistent with the interpretation that those are star-forming galaxies at $z < 1$. Note that, based on the broad-band classification method for emission-line galaxies by Ly et al. (2007), we confirmed that the NB excess of the IA-NB dual-excess objects is consistent with H α emission or [O III] emission. We also confirmed that all of the 10 IA-NB dual-excess objects are detected in the newly obtained U-band data², which strongly supports our conclusions that these IA-NB dual emitters are at $z < 1$.

² The U-band data, obtained recently at the Kitt Peak National Observatory Mayall 4m telescope, are now in the final analysis stages and will be published in a forthcoming paper (Ly et al., in preparation).

Several IA-NB dual emitters have a large ratio of the NB-excess flux to the IA-excess flux, as shown in Table 3. The ratios of the inferred EWs, $EW(\text{IA})$ to $EW(\text{NB})$ estimated following the manner of Fujita et al. (2003b), can be used to obtain rough estimates of the flux ratios of the two emission lines. Ly α -He II dual emitters (i.e., PopIII-hosting galaxies) cannot have such a large flux ratios of He II/Ly α (which should instead be $\lesssim 0.1$, depending on the adopted PopIII models; e.g., Schaerer 2003). In contrast, star-forming galaxies have the flux ratio of [O III]/[O II] ~ 0.1 –10 (depending on the gas metallicity and/or the ionization parameter; e.g., Kewley & Dopita 2002; Nagao et al. 2006) and those of (H α + [N II])/H $\beta \gtrsim 3$ (because the case B flux ratio of H α /H $\beta \sim 3$; e.g., Osterbrock 1989). Therefore, the ratios of the IA excess to the NB excess observed in all IA-NB dual-excess objects are more consistent with the [O III]/[O II] or (H α + [N II])/H β flux ratio of star-forming galaxies at $z < 1$, rather than the He II/Ly α of the PopIII-hosting galaxies.

One interesting object is IA598_117217, that shows only marginal NB excess with a $\sim 2\sigma$ significance. Its $B - V$ color is ~ 1.7 mag, which is consistent with the color of galaxies at $z \sim 4.0$. However, this object has a significant NB921 excess in addition to IA598 and NB816 excess (Figure 8). The corresponding rest-frame wavelength is $\lambda_{\text{rest}} \sim 1840\text{\AA}$ for $z \sim 4.0$ and $\lambda_{\text{rest}} \sim 5641\text{\AA}$ for $z \sim 0.63$, where no strong emission line is expected in either cases. One possibility is that this object harbors an active galactic nucleus (AGN). Since the data of different bands were obtained in different observing runs that span 6 years, the time variation of the AGN may cause a spurious IA and/or NB excess that is not related to emission lines. See, e.g., Morokuma et al. (2008) for the time variation of photometric properties of faint AGNs in deep-survey data. Although the nature of this object is not clear, we do not regard it as a strong candidate of Ly α -He II dual emission at $z \sim 4.0$.

We thus conclude that most of the 10 IA-NB dual emitters found in this survey are [O II]-[O III] or H β -(H α + [N II]) dual emitters, and that photometric candidates of Ly α -He II dual emitters have not been found. Note that the inferred EW_{rest} of them are extremely large (Table 3). Some objects have $EW_{\text{rest}} > 100\text{\AA}$. Although such large-EW objects at $z < 1$ are very rare, some other NB and IA surveys also found such interesting objects (Ajiki et al. 2006; Kakazu et al. 2007). Kakazu et al. (2007) investigated spectra of NB-selected emission-line galaxies with $EW_{\text{rest}} \gtrsim 100\text{\AA}$ and found that some of the targets are extremely metal-poor galaxies (XMPGs, whose oxygen abundance is $12 + \log(\text{O}/\text{H}) < 7.65$; e.g., Kniazev et al. 2003). Since some of our low- z IA-NB dual emitters have similar observational properties as XMPGs, follow-up spectroscopy is of interest.

4. Discussion

In the previous section, we showed that there are neither Ly α -He II dual emitters with $EW_{\text{obs}}(\text{He II}) \gtrsim 45\text{\AA}$ at $3.93 \lesssim z \lesssim 4.01$, nor those with $EW_{\text{obs}}(\text{He II}) \gtrsim 20\text{\AA}$ at $4.57 \lesssim z \lesssim 4.65$, detected in the SDF area at our limiting magnitudes. Here we discuss the implication of these results on the abundance of the PopIII-hosting galaxies at these redshift ranges.

Schaerer (2003) investigated the temporal evolution of $EW(\text{He II})$ for PopIII stellar clusters by assuming IMFs with a Salpeter slope, considering the following three cases; $(M_{\text{low}}, M_{\text{up}}) = (1M_{\odot}, 100M_{\odot})$, $(1M_{\odot}, 500M_{\odot})$, and $(50M_{\odot}, 500M_{\odot})$, where M_{low} and M_{up} are the lower and upper mass cut-off values. Here we focus on the predictions of $EW(\text{He II})$ in the case of $(M_{\text{low}}, M_{\text{up}}) = (50M_{\odot}, 500M_{\odot})$, because numerical simulations suggest IMFs biased toward very high masses (e.g., Bromm et al. 1999; Nakamura & Umemura 2001; Abel et al. 2002; Bromm et al. 2002). Although the predicted $EW(\text{He II})$ reaches $\sim 100\text{\AA}$ at the zero age of the PopIII star formation, it rapidly decreases and becomes undetectable at an age of ~ 2 Myr, if an instantaneous burst is assumed. In the case of constant star-formation, at the equilibrium stage the predicted $EW(\text{He II})$ is $\sim 20\text{\AA}$. This corresponds to $EW_{\text{obs}}(\text{He II}) \sim 100\text{\AA}$ at $z \sim 4.0$ and $EW_{\text{obs}}(\text{He II}) \sim 110\text{\AA}$ at $z \sim 4.6$ (or equivalently, a NB excess of ~ 0.6 mag for both redshift ranges), which are much larger than the detection limit of our observation. This suggests that PopIII-hosting galaxies younger than ~ 2 Myr or having on-going PopIII-formation, with an enough high star-formation rate (SFR_{PopIII}), should be detected in our surveys.

In the following we quantify the minimum SFR_{PopIII} to which our survey is sensitive. By assuming constant star formation, the He II luminosity can be written as follows:

$$L(\text{HeII}) = (1 - f_{\text{esc}})f_{1640} \left(\frac{SFR_{\text{PopIII}}}{M_{\odot}\text{yr}^{-1}} \right), \quad (11)$$

where f_{esc} is the escape fraction of the He^+ -ionizing photon and f_{1640} is a proportionality constant. In the following we assume that f_{esc} is negligibly small. Schaerer (2003) predicted $f_{1640} = 6.01 \times 10^{41}$ for PopIII stellar clusters with $(M_{\text{low}}, M_{\text{up}}) = (50M_{\odot}, 500M_{\odot})$. This corresponds to $F(\text{He II}) = 3.91 \times 10^{-18}$ ($SFR_{\text{PopIII}}/M_{\odot} \text{ yr}^{-1}$) for $z = 4.0$ and $F(\text{He II}) = 2.81 \times 10^{-18}$ ($SFR_{\text{PopIII}}/M_{\odot} \text{ yr}^{-1}$) for $z = 4.6$, in units of $\text{erg s}^{-1} \text{ cm}^{-2}$. Since the 3σ limiting flux of objects with $EW_{\text{obs}} = 100\text{\AA}$ in our NB816 observation is $7.4 \times 10^{-18} \text{ erg s}^{-1} \text{ cm}^{-2}$ and that of objects with $EW_{\text{obs}} = 110\text{\AA}$ in our NB921 observation is $5.9 \times 10^{-18} \text{ erg s}^{-1} \text{ cm}^{-2}$, our survey can detect PopIII-hosting galaxies if their SFR is higher than $\sim 2M_{\odot} \text{ yr}^{-1}$. Therefore, the non-detection of $\text{Ly}\alpha$ -He II dual emitters suggests that there are no PopIII-hosting galaxies with $SFR_{\text{PopIII}} \gtrsim 2M_{\odot} \text{ yr}^{-1}$ at $4.0 \lesssim z \lesssim 4.6$ toward the SDF, in a volume of $4.03 \times 10^5 \text{ Mpc}^3$. This result implies an upper-limit of the PopIII SFR density of $SFRD_{\text{PopIII}} < 5 \times 10^{-6} M_{\odot} \text{ yr}^{-1} \text{ Mpc}^{-3}$, if taking only galaxies with $SFR_{\text{PopIII}} > 2M_{\odot} \text{ yr}^{-1}$ into account. Note that the inferred upper limit on SFR_{PopIII} is uncertain, since the predicted flux of He II for a given SFR_{PopIII} strongly depends on the assumed IMF (e.g., Schaerer 2003). It also depends on the evolutionary processes of PopIII stars, especially the mass loss during their evolution (e.g., El Eid et al. 1983; Tumlinson et al. 2001; Schaerer 2002).

Some theoretical studies suggest that the volume-averaged IGM metallicity quickly reached $Z_{\text{crit}} = 10^{-4}Z_{\odot}$ at $z > 10$ (e.g., Mackey et al. 2003; Yoshida et al. 2004; Tornatore et al. 2007), where Z_{crit} is the critical metallicity, below which very massive stars could be formed. However, this does not necessarily suggest that the formation of PopIII stars was terminated at such a high redshift, because of the inhomogeneous metal distribution in the early universe (e.g., Scannapieco et al. 2003, 2006; Brook et al. 2007; Tornatore et al. 2007). As demonstrated by Scannapieco

et al. (2003), the redshift evolution of the SFR_{PopIII} density in the universe depends sensitively on some PopIII model parameters, especially the feedback efficiency that is closely related to the PopIII IMF (see also Scannapieco et al. 2006). Low-feedback models of Scannapieco et al. (2003) predict a large fraction ($\sim 30\%$) of PopIII-hosting galaxies among LAEs at $4.0 \lesssim z \lesssim 4.6$ with $\log L(\text{Ly}\alpha) \sim 10^{43} \text{ ergs s}^{-1}$ (again $M_{\text{low}} = 50M_{\odot}$ is assumed here). A similarly large fraction of PopIII-hosting galaxies among high- z LAEs is also inferred by Dijkstra & Wyithe (2007). Since the number density of LAEs with this luminosity at similar redshifts is $\sim 10^{-5} - 10^{-4} \text{ Mpc}^{-3}$ (Ouchi et al. 2003; Yamada et al. 2005; Ouchi et al. 2008), the number of PopIII-hosting galaxies in our survey, expected by such low-feedback models, is roughly 1 to 10. Therefore, the non-detection in our “Ly α -He II dual emitters” survey may suggest that low-feedback models are not appropriate, and that PopIII stars may instead be characterized by a relatively large feedback efficiency.

This photometric survey for Ly α -He II dual emitters demonstrated that wide and deep imaging observations, combining narrow-band and/or intermediate-band filters, are potentially a powerful tool to search or constrain the properties of PopIII-hosting galaxies at high redshifts. The data recently obtained by sensitive narrow-band near-infrared surveys at $1.19\mu\text{m}$ (Willis & Courbin 2005; Cuby et al. 2007; Willis et al. 2007) and similar wide and deep surveys planned in future may be useful to search for Ly α -He II dual emitters at $z \sim 6.3$, by adding data of narrow- or intermediate-band observations at $\lambda \sim 8820\text{\AA}$ to check strong Ly α emission. Such a survey is promising, since SFR_{PopIII} increases at higher redshifts (see, e.g., Dijkstra & Wyithe 2007). In future observational searches for Ly α -He II dual emitters, serious sources of contamination would be [O II]-[O III] and H β -(H α + [N II]) dual emitters, as demonstrated in this paper. In addition to broad-band color criteria, the flux (or EW) ratio of the dual excesses is also a powerful diagnostic to discriminate the populations and to identify Ly α -He II dual emitters among the photometric candidates.

We thank A. Marconi, K. Shimasaku, M. Morokuma, T., Yagi, K. Omukai, N. Yoshida, and the anonymous referee for their useful comments, and Y. Ideue, S. Mihara and A. Nakajima for assisting the Subaru observation runs. We also thank K. Ota for providing us an optical sky spectrum. This research is based on data collected at the Subaru Telescope, which is operated by the National Astronomical Observatory of Japan. We are grateful to all members of the Subaru Deep Field project and to the staff of the Subaru Telescope, especially to the Subaru support astronomers, H. Furusawa and M. Takami. We wish to recognize and acknowledge the very significant cultural role and relevance that the summit of Mauna Kea has always had within the indigenous Hawaiian community. We are most fortunate to have the opportunity to conduct observations from this mountain. TN and SSS are financially supported by the Japan Society for the Promotion of Science (JSPS) through JSPS Research Fellowship for Young Scientists.

REFERENCES

Abel, T., Bryan, G. K., & Norman, M. L. 2002, *Science*, 295, 93

- Abia, C., Domínguez, I., Straniero, O., et al. 2001, *ApJ*, 557, 126
- Ajiki, M., Taniguchi, Y., Fujita, S. S., et al. 2003, *AJ*, 126, 2091
- Ajiki, M., Taniguchi, Y., Fujita, S. S., et al. 2004, *PASJ*, 56, 597
- Ajiki, M., Shioya, Y., Taniguchi, Y., et al. 2006, *PASJ*, 58, 113
- Bertin, E., & Arnouts, S. 1996, *A&AS*, 117, 393
- Bromm, V., Coppi, P. S., & Larson, R. B. 1999, *ApJ*, 527, L5
- Bromm, V., Coppi, P. S., & Larson, R. B. 2002, *ApJ*, 564, 23
- Bromm, V., Kudritzki, R. P., & Loeb, A. 2001, *ApJ*, 552, 464
- Bromm, V., Yoshida, N., & Hernquist, L. 2003, *ApJ*, 596, L135
- Brook, C. B., Kawata, D., Scannapieco, E., et al. 2007, *ApJ*, 661, 10
- Bruzual, G., & Charlot, S. 2003, *MNRAS*, 344, 1000
- Cardelli, J. A., Clayton, G. C., & Mathis, J. S. 1989, *ApJ*, 345, 245
- Ciardi, B., Ferrara, A., Governato, F., & Jenkins, A., 2000, *MNRAS*, 314, 611
- Cuby, J. -G., Hibon, P., Lidman, C., et al. 2007, *A&A*, 461, 911
- Dawson, S., Rhoads, J. E., Malhotra, S., et al. 2004, *ApJ*, 617, 707
- Dijkstra, M., & Wyithe, J. S. B. 2007, *MNRAS*, 379, 1589
- El Eid, M. F., Fricke, K. J., & Ober, W. W. 1983, *A&A*, 119, 54
- Fujita, S. S., Ajiki, M., Shioya, Y., et al. 2003a, *AJ*, 125, 13
- Fujita, S. S., Ajiki, M., Shioya, Y., et al. 2003b, *ApJ*, 586, L115
- Iye, M., Karoji, H., Ando, H., et al. 2004, *PASJ*, 56, 381
- Iye, M., Ota, K., Kashikawa, N., et al. 2006, *Nature*, 443, 186
- Jimenez, R., & Haiman, Z. 2006, *Nature*, 441, 120
- Kakazu, Y., Cowie, L. L., & Hu, E. M. 2007, *ApJ*, 668, 853
- Kashikawa, N., Shimasaku, K., Yasuda, N., et al. 2004, *PASJ*, 56, 1011
- Kashikawa, N., Shimasaku, K., Malkan, M. A., et al. 2006, *ApJ*, 648, 7
- Kewley, L. J., & Dopita, M. A. 2002, *ApJS*, 142, 35

- Kodaira, K., Taniguchi, Y., Kashikawa, N., et al. 2003, PASJ, 55, L17
- Kuniazhev, A. Y., Grebel, E. K., Hao, L., et al. 2003, ApJ, 593, L73
- Loeb, A., & Barkana, R. 2001, ARA&A, 39, 19
- Ly, C., Malkan, M. A., Kashikawa, N., et al. 2007, ApJ, 657, 738
- Mackey, J., Bromm, V., & Hernquist, L. 2003, ApJ, 586, 1
- Madau, P., Ferguson, H. C., Dickinson, M. E., et al. 1996, MNRAS, 283, 1388
- Malhotra, S., & Rhoads, J. E. 2002, ApJ, 565, L71
- Miyazaki, S., Komiyama, Y., Sekiguchi, M., et al. 2002, PASJ, 54, 833
- Morokuma, T., Doi M., Yasuda, N., et al. 2008, ApJ, in press (arXiv:0712.3106)
- Nagao, T., Kashikawa, N., Malkan, M. A., et al. 2005a, ApJ, 634, 142
- Nagao, T., Maiolino, R., & Marconi, A. 2006, A&A, 459, 85
- Nagao, T., Motohara, K., Maiolino, R., et al. 2005b, ApJ, 631, L5
- Nagao, T., Murayama, T., Maiolino, R., et al. 2007, A&A, 468, 877
- Nagao, T., Taniguchi, Y., Kashikawa, N., et al. 2004, ApJ, 613, L9
- Nakamura, F., & Umemura, M. 2001, ApJ, 548, 19
- Oh, S. P., Haiman, Z., & Rees, M. J. 2001, ApJ, 553, 73
- Osterbrock, D. E. 1989, Astrophysics of Gaseous Nebulae and Active Galactic Nuclei (Mill Valley: University Science Books)
- Ota, K., Iye, M., Kashikawa, N., et al. 2007, ApJ, submitted (arXiv.0707.1561)
- Ouchi, M., Shimasaku, K., Akiyama, M., et al. 2008, ApJS, in press (arXiv.0707.3161)
- Ouchi, M., Shimasaku, K., Furusawa, H., et al. 2003, ApJ, 582, 60
- Ouchi, M., Shimasaku, K., Okamura, S., et al. 2004, ApJ, 611, 660
- Qian, Y. -Z. & Wasserburg, G. J. 2001, ApJ, 549, 337
- Scannapieco, E., Kawata, D., Brook, C. B., et al. 2006, ApJ, 653, 285
- Scannapieco, E., Schneider, R., & Ferrara, A. 2003, ApJ, 589, 35
- Schaerer, D. 2002, A&A, 382, 28

- Schaerer, D. 2003, *A&A*, 397, 527
- Schlegel, D. J., Finkbeiner, D. P., & Davis, M. 1998, *ApJ*, 500, 525
- Schneider, R., Salvaterra, R., Ferrara, A., & Ciardi, B. 2006, *MNRAS*, 369, 825
- Shapley, A. E., Steidel, C. C., Pettini, M., & Adelberger, K. L. 2003, *ApJ*, 588, 65
- Shimasaku, K., Hayashino, T., Matsuda, Y., et al. 2004, *ApJ*, 605, L93
- Shimasaku, K., Kashikawa, N., Doi, M., et al. 2006, *PASJ*, 58, 313
- Shimasaku, K., Ouchi, M., Okamura, S., et al. 2003, *ApJ*, 586, L111
- Sokasian, A., Yoshida, N., Abel, T., Hernquist, L., & Springel, V. 2004, *MNRAS*, 350, 47
- Taniguchi, Y., Ajiki, M., Nagao, T., et al. 2005a, *PASJ*, 57, 165
- Taniguchi, Y., Scoville, N. Z., Sanders, D. B., et al. 2005b, *JKAS*, 38, 187
- Tornatore, L., Ferrara, A., & Schneider, R. 2007, *MNRAS*, 382, 945
- Tumlinson, J., Giroux, M. L., & Shull, J. M. 2001, *ApJ*, 550, L1
- Tumlinson, J., & Shull, J. M. 2000, *ApJ*, 528, L65
- Tumlinson, J., & Shull, J. M., & Venkatesan, A. 2003, *ApJ*, 584, 608
- Wasserburg, G. J., & Qian, Y. -Z. 2000, *ApJ*, 538, L99
- Willis, J. P., & Courbin, F. 2005, *MNRAS*, 357, 1348
- Willis, J. P., Courbin, F., Kneib, J. P., & Minniti, D. 2007, *MNRAS*, in press (arXiv.0709.1761)
- Wyithe, J. S. B., & Loeb, A. 2003, *ApJ*, 586, 693
- Yagi, M., Kashikawa, N., Sekiguchi, M., et al. 2002, *AJ*, 123, 66
- Yamada, S. F., Sasaki, S. S., Sumiya, R., et al. 2005, *PASJ*, 57, 881
- Yoshida, N., Bromm, V., & Hernquist, L. 2004, *ApJ*, 605, 579

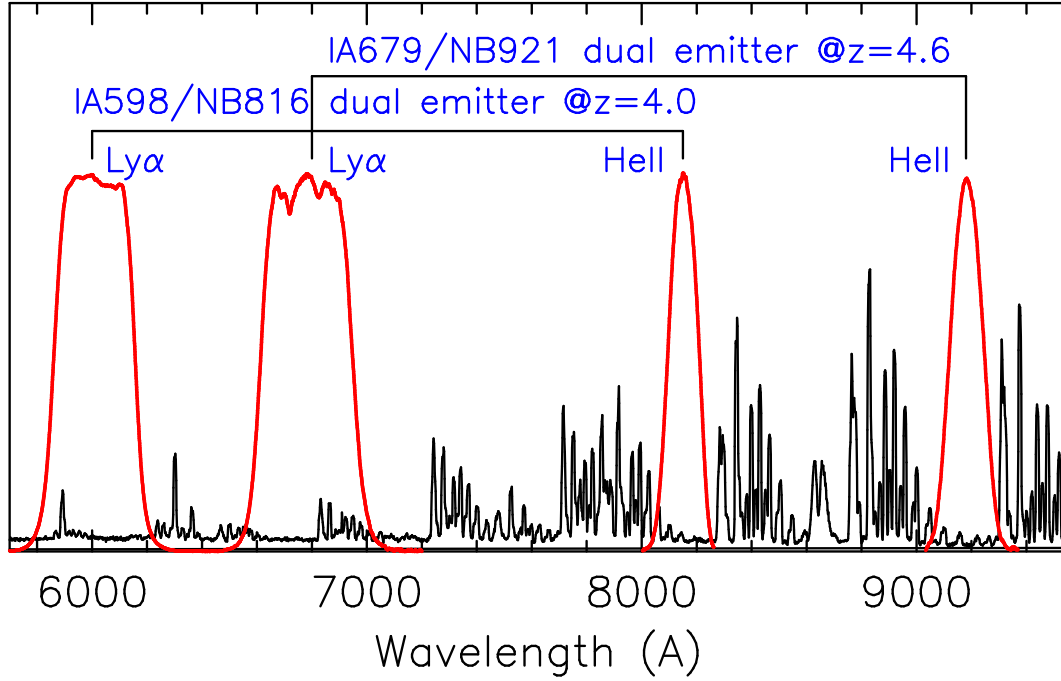


Fig. 1.— Schematic view of the selection of Ly α -He II dual emitters. The black solid spectrum denotes a typical background sky spectrum. Red solid curves denote the filter transmission curves of IA598, IA679, NB816, and NB921. The dual excess of the combination of IA598 and NB816, and that of IA679 and NB921 correspond to $z \sim 4.0$ and $z \sim 4.6$, respectively.

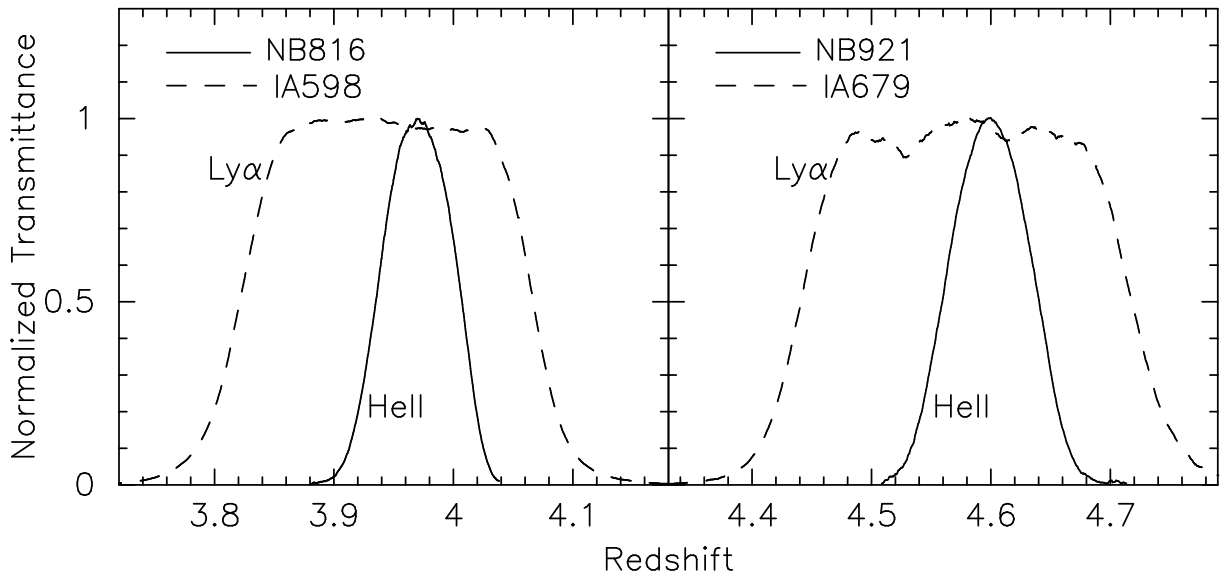


Fig. 2.— Transmission curves of IA598 and NB816 (dashed and solid lines in the left panel), and those of IA679 and NB921 (dashed and solid lines in the right panel) normalized by their peak transmittances are shown as a function of redshift.

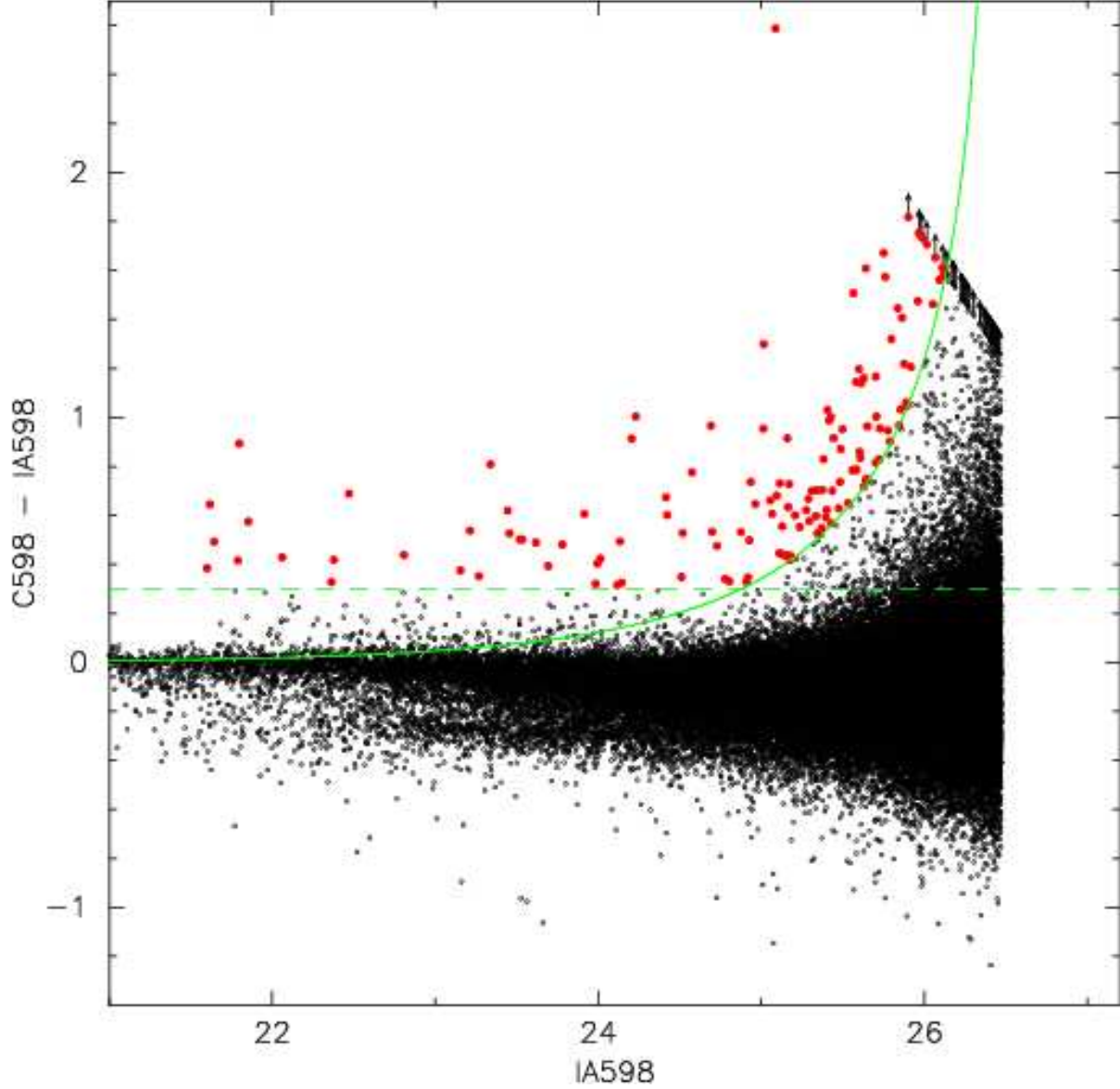


Fig. 3.— IA598-detected objects (which are also detected at 2σ in both R_C and i' images), plotted on a diagram of $C598-IA598$ vs $IA598$ (black dots; 63660 objects). The dashed green horizontal line denotes the excess criterion limit, $C598-IA598 = 0.3$. The solid green curve denotes 3σ uncertainty in the $C598-IA598$ color. Objects with a lower-limit on the color of $C598-IA598$ are shown with arrows. Red, filled circles denote the selected IA598-excess galaxies (133 objects).

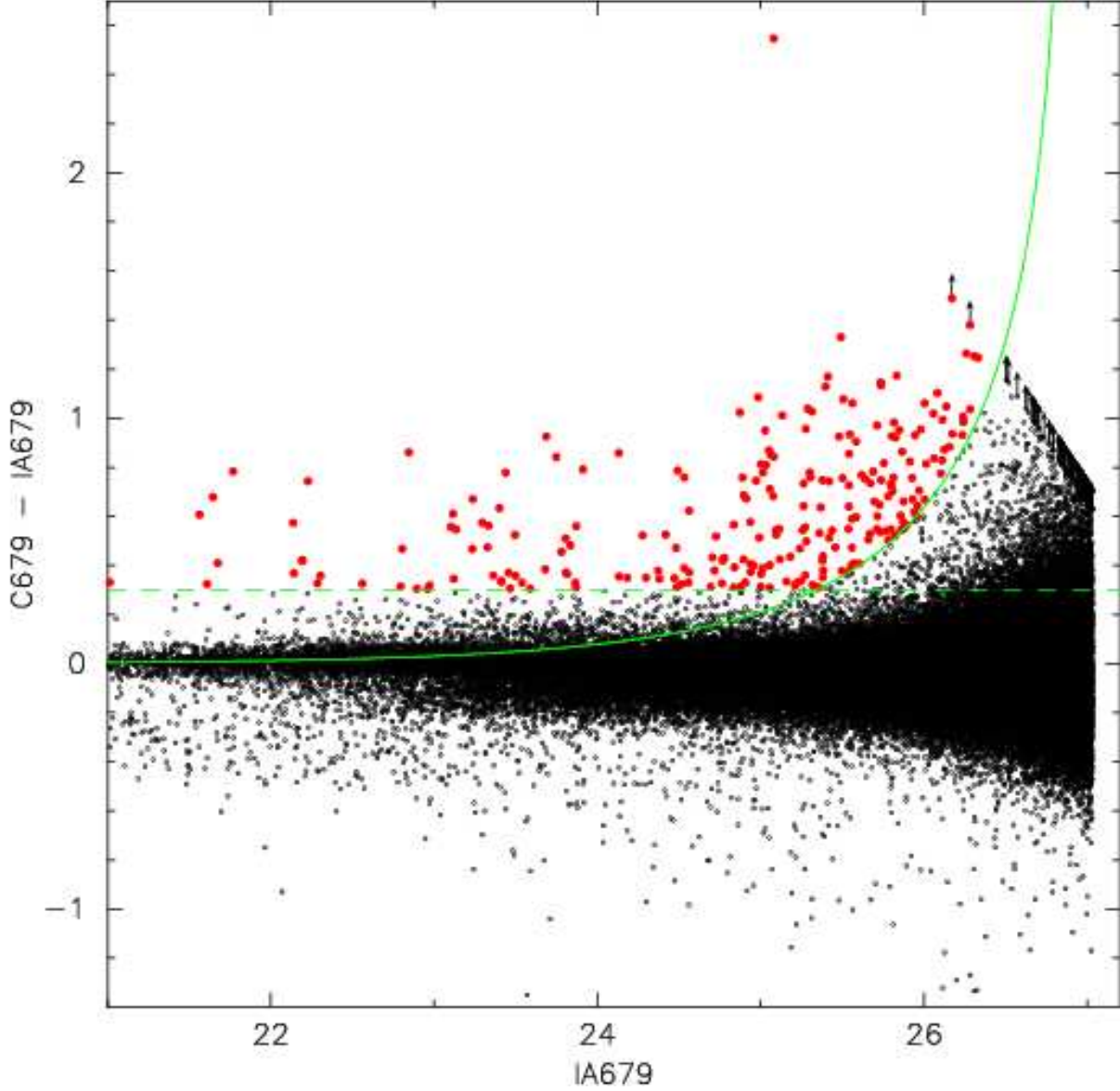


Fig. 4.— IA679-detected objects (which are also detected at 2σ in both R_C and i' images), plotted on a diagram of $C679-IA679$ vs $IA679$ (black dots; 97234 objects). The dashed green horizontal line denotes the excess criterion limit, $C679-IA679 = 0.3$. The solid green curve denotes 3σ uncertainty in the $C679-IA679$ color. Objects with a lower-limit on the color of $C679-IA679$ are shown with arrows. Red, filled circles denote the selected IA679-excess galaxies (234 objects).

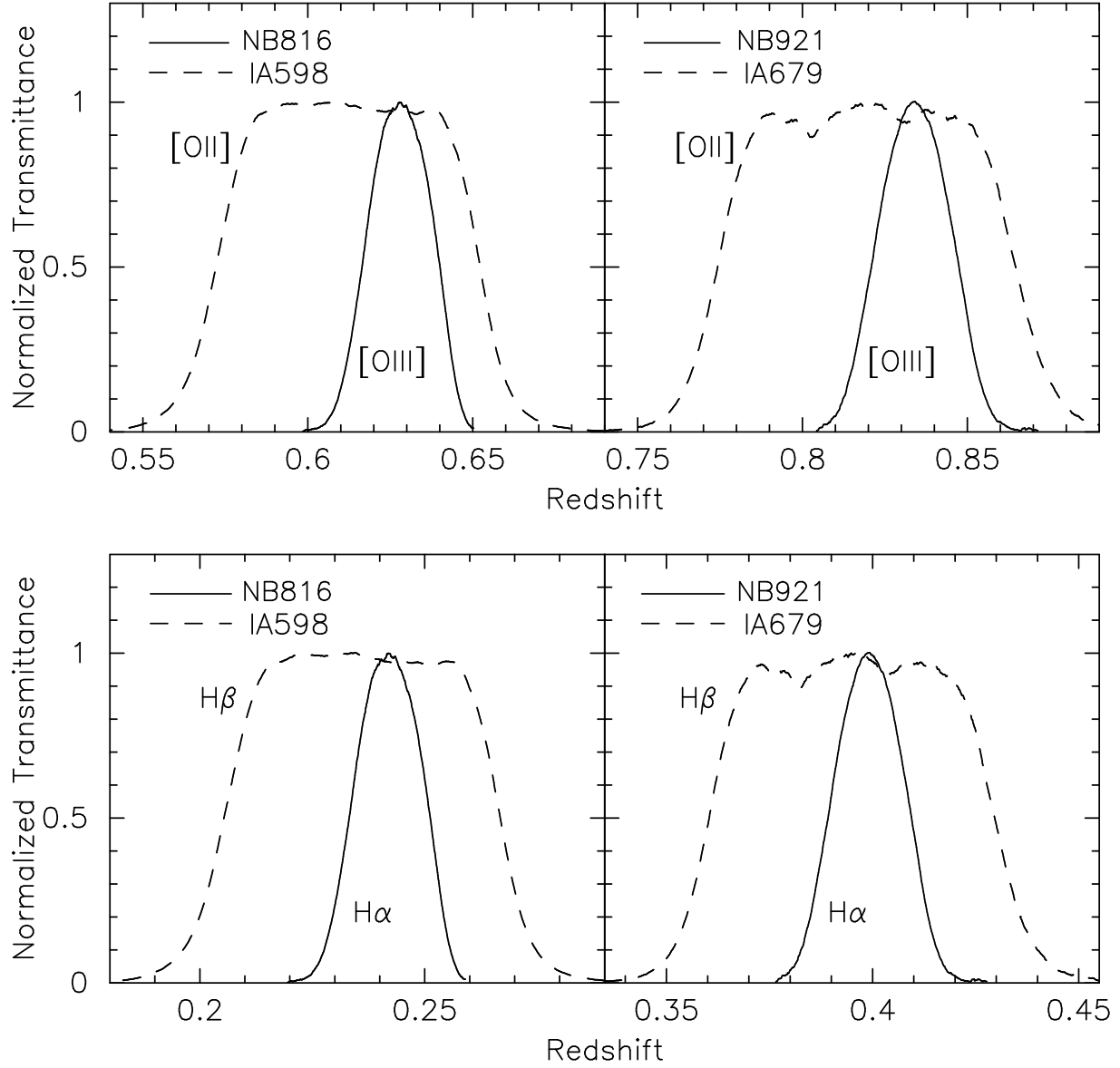


Fig. 5.— Same as Figure 2 but for [O II]-[O III] dual emitters (upper panels) and for H β -(H α + [N II]) dual emitters (lower panels).

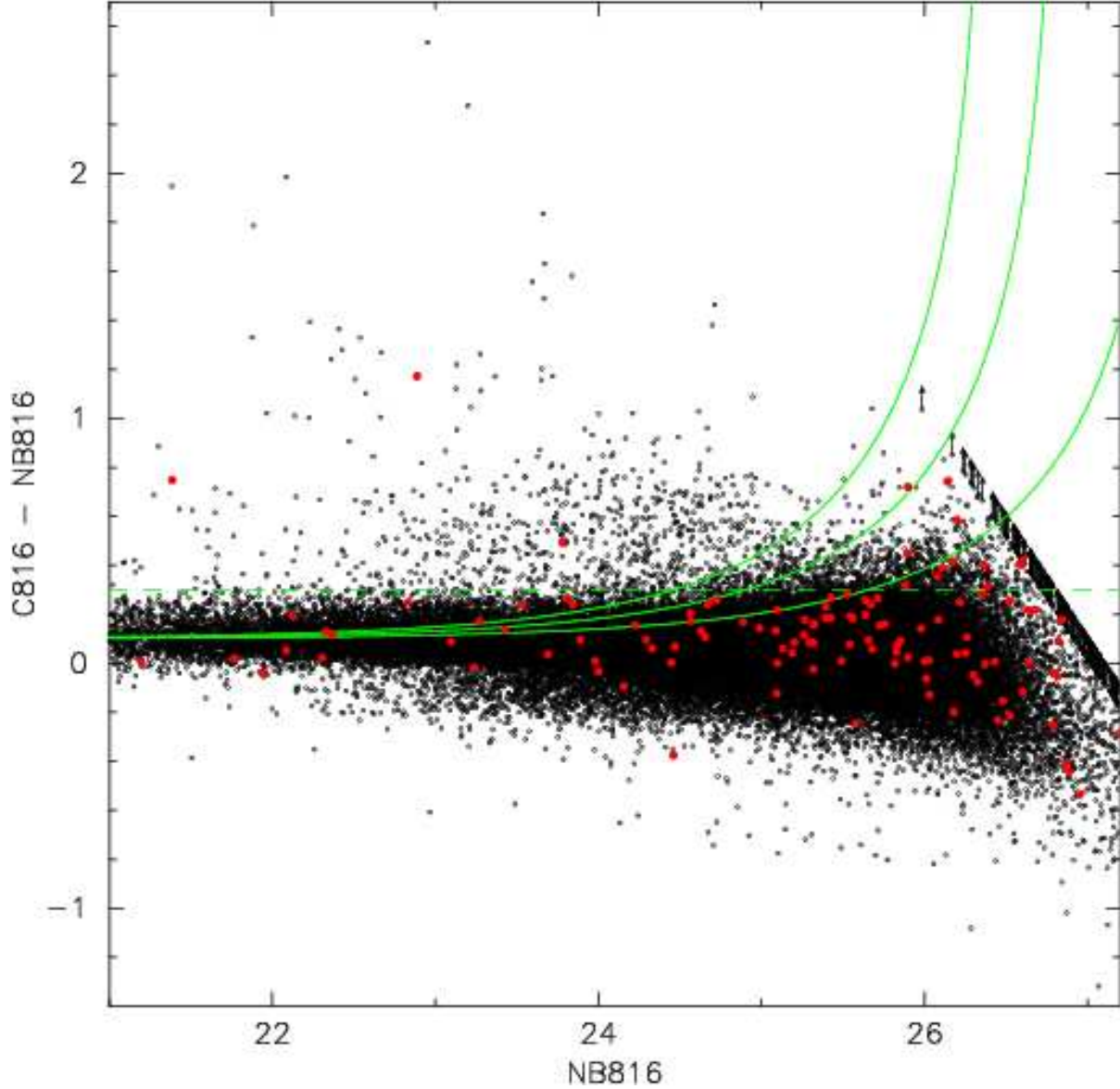


Fig. 6.— IA598-detected objects (which are also detected at 2σ in both R_C and i' images), plotted on a diagram of $C816 - NB816$ vs $NB816$ (black dots; 63660 objects). The dashed green horizontal line denotes the excess criterion limit, $C816 - NB816 = 0.3$. The solid green curve denotes 3σ , 2σ , and 1σ uncertainty in the $C816 - NB816$ color, taking a $+0.10$ mag offset into account (see text). Objects with a lower-limit on the color of $C816 - IA816$ are shown with arrows. Red, filled circles denote the selected IA598-excess galaxies (133 objects).

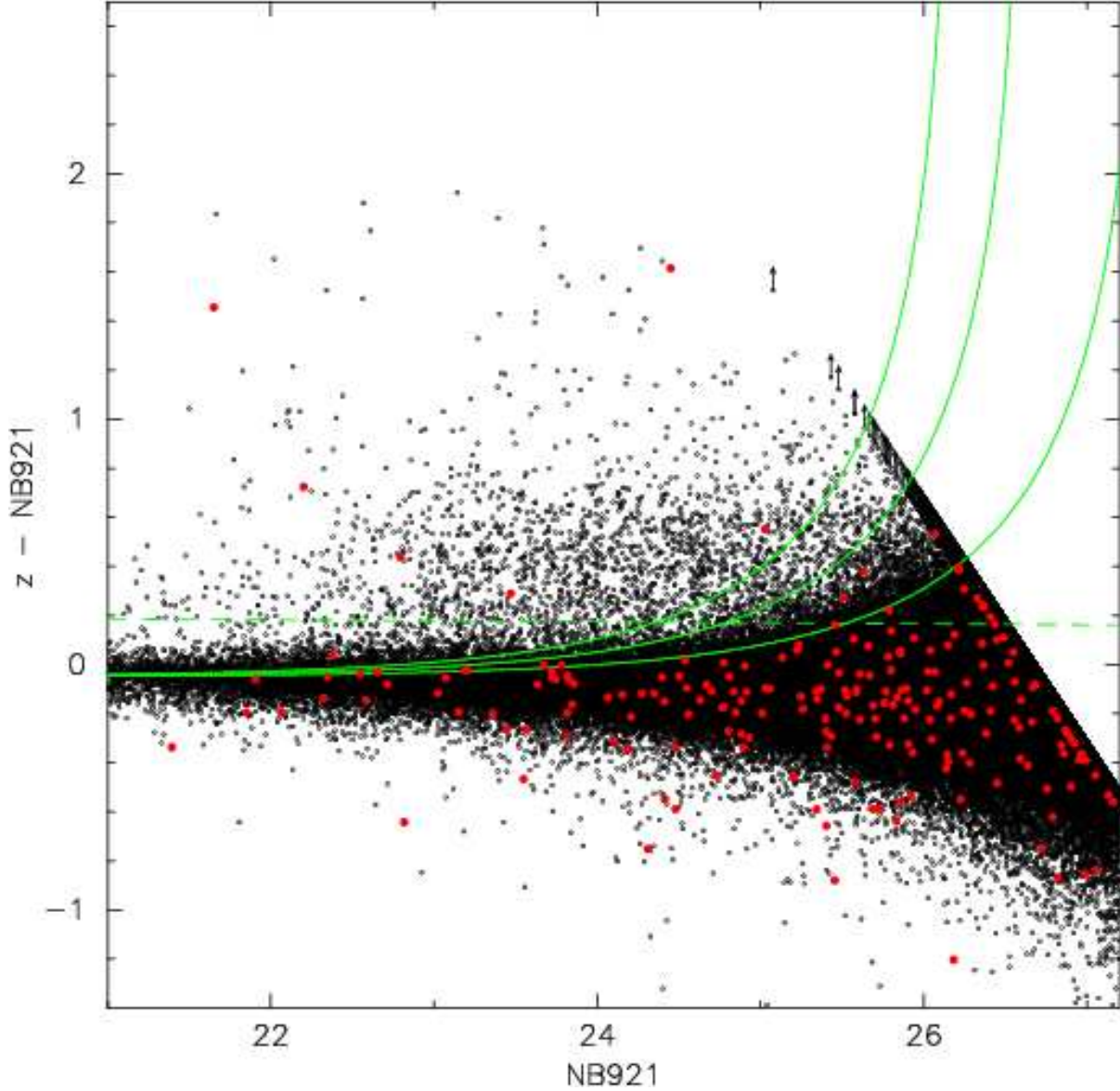


Fig. 7.— IA679-detected objects (which are also detected at 2σ in both R_C and i' images), plotted on a diagram of $z' - NB921$ vs $NB921$ (black dots; 97234 objects). The dashed green horizontal line denotes the excess criterion limit, $z' - NB921 = 0.3$. The solid green curve denotes 3σ , 2σ , and 1σ uncertainty in the $z' - NB921$ color, taking a -0.05 mag offset into account (see text). Objects with a lower-limit on the color of $z' - NB921$ are shown with arrows. Red, filled circles denote the selected IA679-excess galaxies (234 objects).

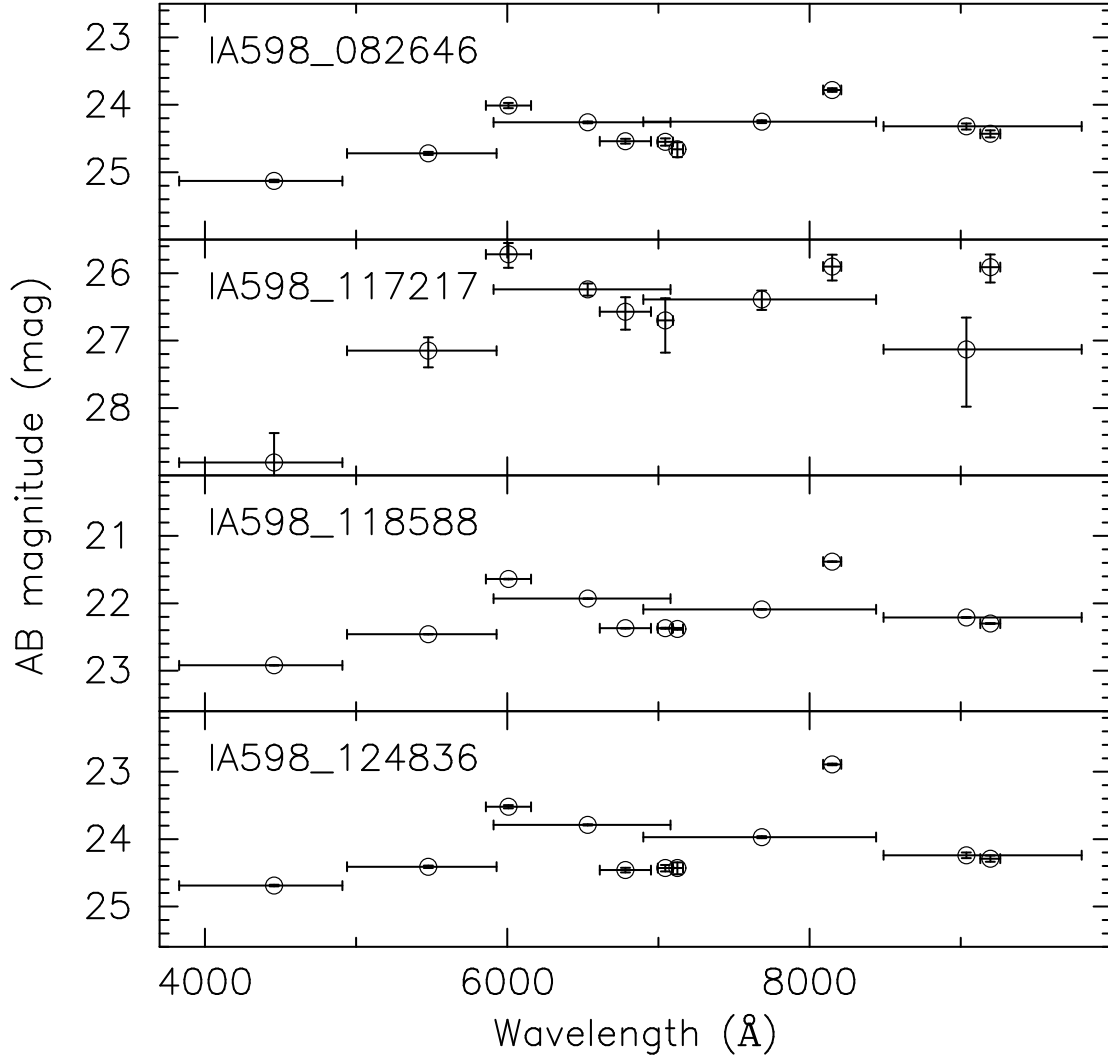


Fig. 8.— SEDs of the IA598-NB816 dual emitters. Error bars in the y-axis direction denote the 1σ photometric errors. The ID of each object is shown at the upper-left corner of each panel.

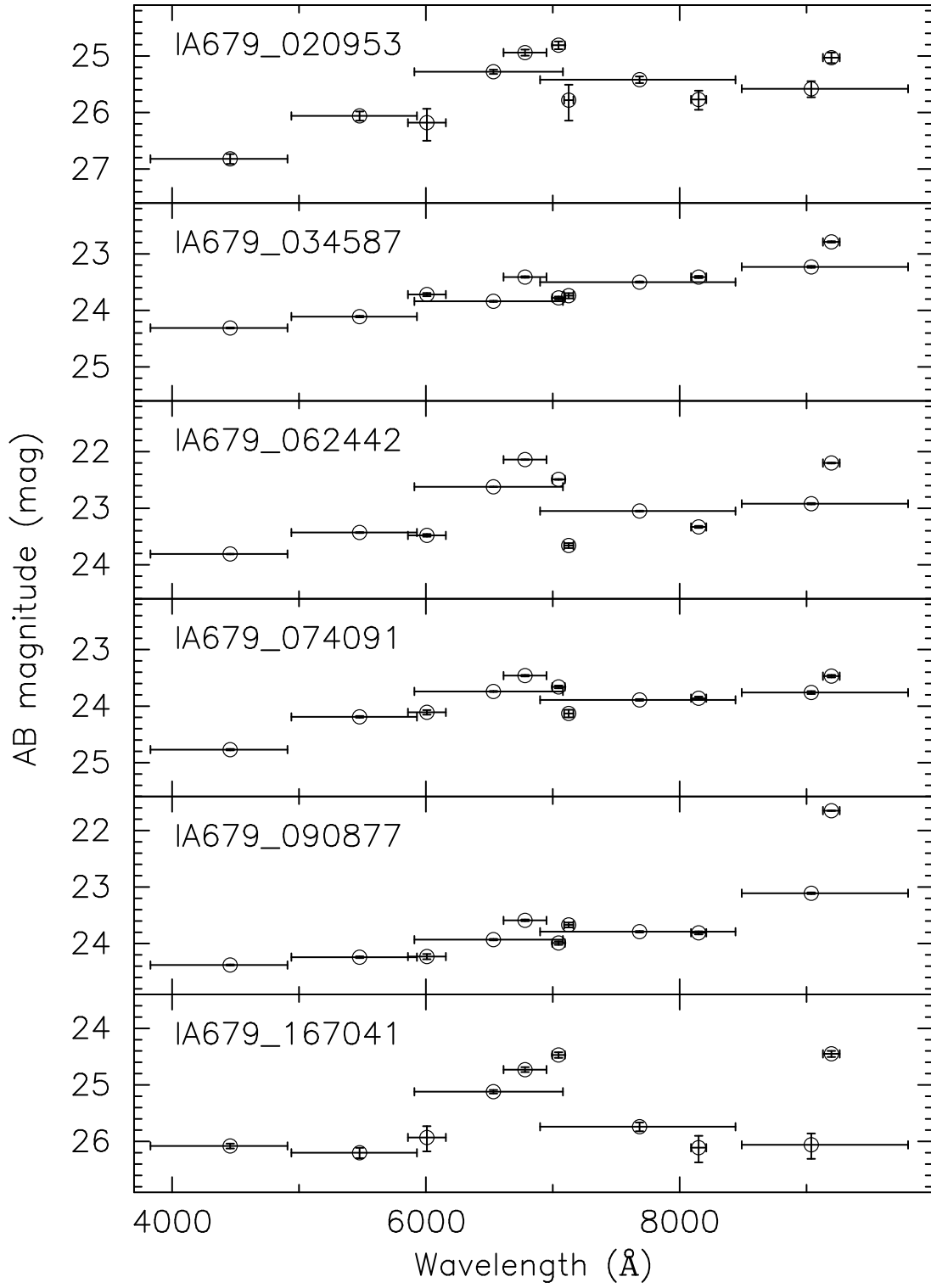


Fig. 9.— Same as Figure 8 but for the IA679-NB921 dual emitters.

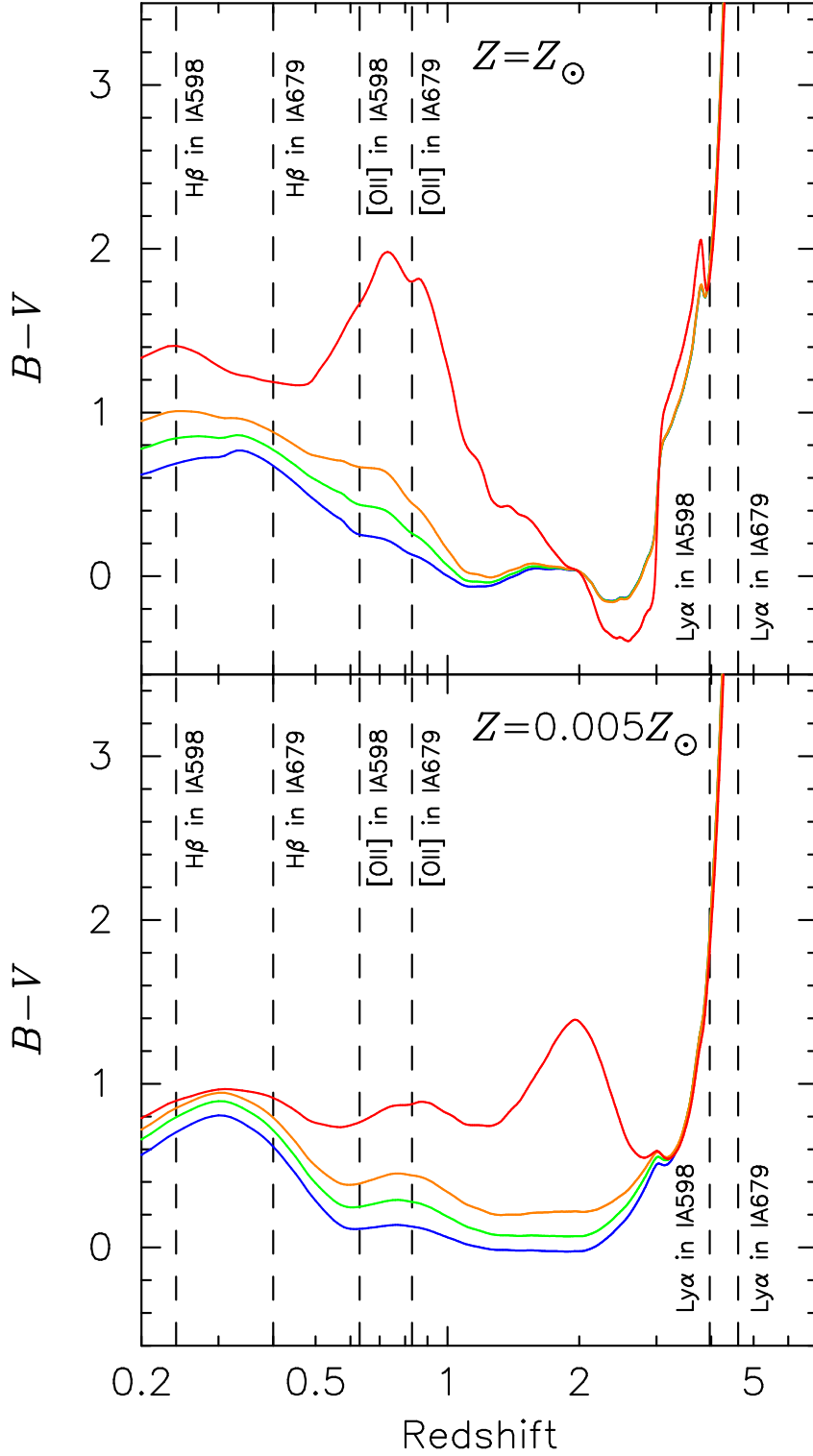


Fig. 10.— Predicted $B - V$ color of galaxy models (Bruzual & Charlot 2003) as a function of redshift. The galaxy models have Salpeter IMF and an exponentially declining star-formation history with $\tau = 1$ Gyr. Blue, green, yellow, and red solid lines corresponds to the model predictions for an age of 2, 3, 4, and 8 Gyr, respectively. Vertical dashed lines denote the redshifts where the IA-NB dual-excess objects are expected to be located. Models with a metallicity of $Z = Z_{\odot}$ and with that of $Z = 0.005 Z_{\odot}$ are shown in the upper and lower panels, respectively.

Table 1. Available optical photometric data in the SDF

Filter	t_{exp} (min.)	$m_{\text{lim}}^{\text{a}}$ (mag)	A_V^{b} (mag)	Ref. ^c
B	595	28.45	0.07	1
V	340	27.74	0.05	1
R_C	600	27.80	0.04	1
i'	801	27.43	0.03	1
z'	504	26.62	0.02	1
IA598	111	26.52	0.05	2
IA679	231	27.07	0.04	2
NB704	198	26.67	0.04	3, 4
NB711	162	25.99	0.04	4, 5, 6
NB816	600	26.63	0.03	1, 4, 7
NB921	899	26.54	0.02	1, 4, 8, 9, 10
NB973	900	25.5	0.02	11, 12

^a 3σ limiting magnitude for $2''\phi$ apertures, without the Galactic reddening correction.

^bGalactic extinction for each band (Schlegel et al. 1998), calculated by adopting the Galactic extinction curve (Cardelli et al. 1989).

^cReferences: (1) Kashikawa et al. (2004). (2) This work. (3) Shimasaku et al. (2004). (4) Ly et al. (2007). (5) Ouchi et al. (2003). (6) Shimasaku et al. (2003). (7) Shimasaku et al. (2006). (8) Kodaira et al. (2003). (9) Taniguchi et al. (2005a). (10) Kashikawa et al. (2006). (11) Iye et al. (2006). (12) Ota et al. (2007).

Table 2. Photometric properties of IA-NB dual emitters^a

ID	B (mag)	V (mag)	R_C (mag)	i' (mag)	z' (mag)	IA598 (mag)	IA679 (mag)	NB704 (mag)	NB711 (mag)	NB816 (mag)	NB921 (mag)
IA598_082646	25.13	24.72	24.26	24.25	24.32	24.01	24.54	24.55	24.66	23.78	24.43
IA598_117217	28.81	27.15	26.24	26.39	27.13	25.72	26.57	26.70	—	25.90	25.91
IA598_118588	22.92	22.46	21.93	22.09	22.21	21.64	22.37	22.37	22.38	21.38	22.30
IA598_124836	24.69	24.41	23.79	23.97	24.24	23.52	24.46	24.43	24.43	22.89	24.29
IA679_020953	26.82	26.06	25.28	25.42	25.58	26.18	24.94	24.81	25.78	25.77	25.03
IA679_034587	24.31	24.11	23.84	23.50	23.23	23.72	23.41	23.78	23.74	23.41	22.79
IA679_062442	23.81	23.43	22.62	23.05	22.92	23.48	22.14	22.49	23.66	23.33	22.20
IA679_074091	24.77	24.19	23.74	23.89	23.76	24.11	23.46	23.66	24.13	23.86	23.47
IA679_090877	24.38	24.24	23.93	23.79	23.11	24.23	23.59	23.99	23.67	23.81	21.65
IA679_167041	26.08	26.20	25.12	25.74	26.06	25.93	24.73	24.47	—	26.11	24.45

^aCorrected for the Galactic extinction.

Table 3. Equivalent widths of IA-NB dual emitters

ID	$EW_{\text{obs}}(\text{IA})$ (Å)	$EW_{\text{obs}}(\text{NB})$ (Å)
IA598_082646	181 ± 20	83 ± 8
IA598_117217	483 ± 157	137 ± 67
IA598_118588	218 ± 2	147 ± 1
IA598_124836	224 ± 14	299 ± 6
IA679_020953	191 ± 37	96 ± 28
IA679_034587	167 ± 9	72 ± 3
IA679_062442	349 ± 4	141 ± 2
IA679_074091	154 ± 9	43 ± 5
IA679_090877	147 ± 10	542 ± 4
IA679_167041	297 ± 36	709 ± 62